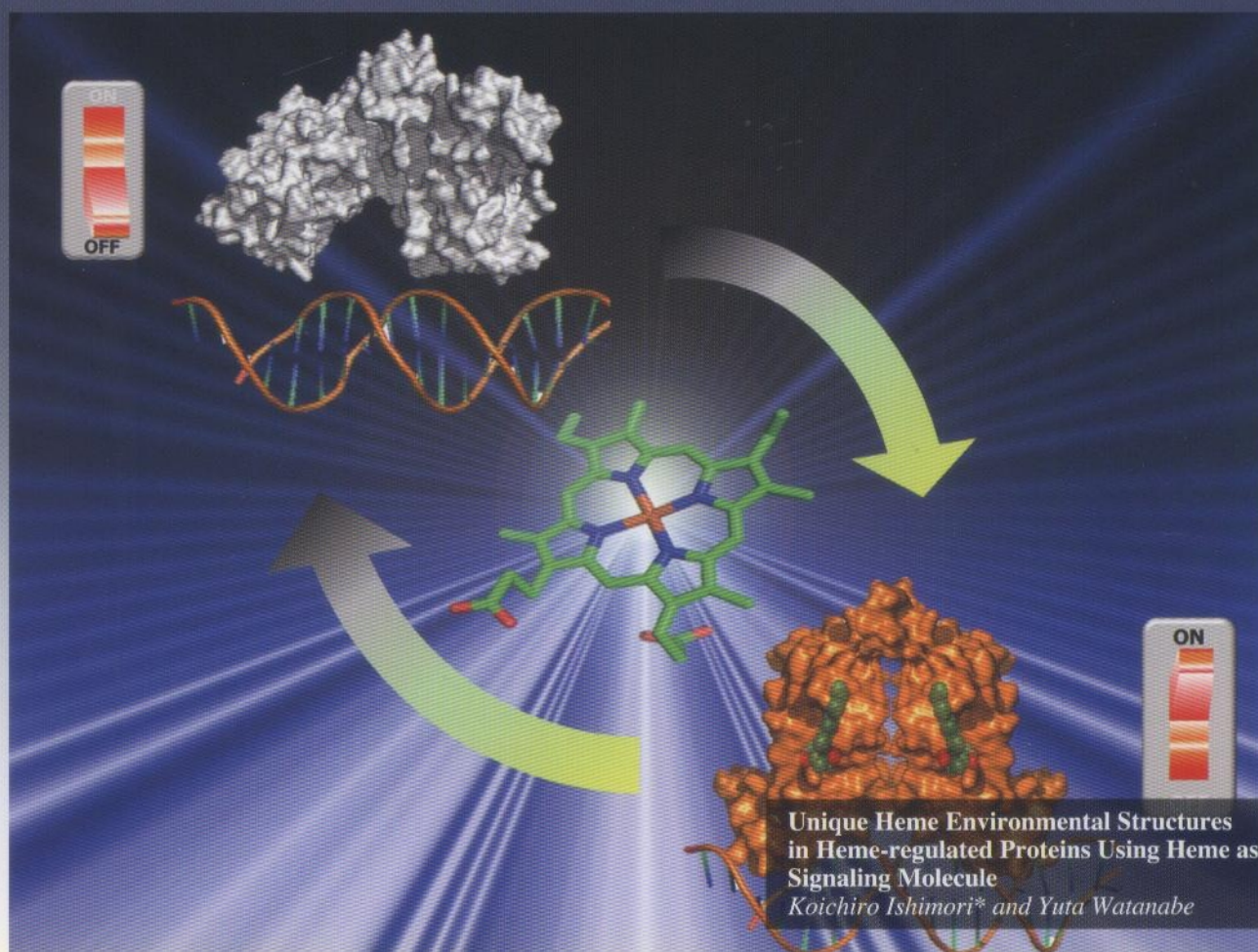


Chemistry Letters



Vol. 43 No. 11 2014

CMLTAG

1671-1814 (2014)

NOVEMBER 5, 2014

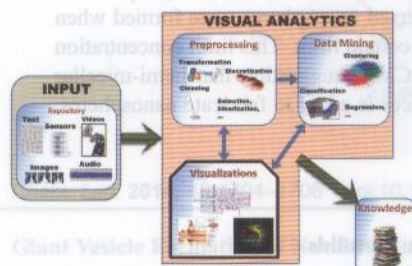


The Chemical Society of Japan

Highlight Review

Where Chemical Sensors May Assist in Clinical Diagnosis Exploring “Big Data”

Osvaldo N. Oliveira, Jr.,* Tácio T. A. T. Neves,
Fernando V. Paulovich, and Maria Cristina F. de Oliveira



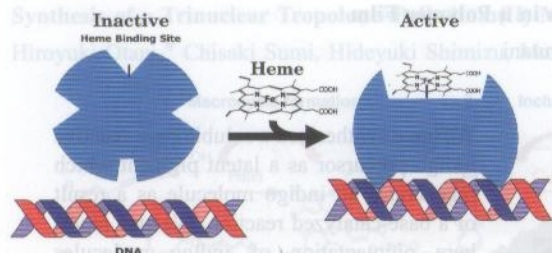
Framework of an expert system for clinical diagnosis, where computational methods of different kinds are integrated to exploit “Big Data” concepts. Datasets are expected to be obtained from the patient being considered and from a repository built for a large number of other patients. Such datasets will be obtained from chemical sensors, biosensors, imaging systems, and patient records. All of these data will be manipulated with a variety of methods indicated in the boxes of the flowchart, in order to reach an informed diagnostics.

Chem. Lett. 2014, 43 1672–1679 doi:10.1246/cl.140762

Highlight Review

Unique Heme Environmental Structures in Heme-regulated Proteins Using Heme as the Signaling Molecule

Koichiro Ishimori* and Yuta Watanabe

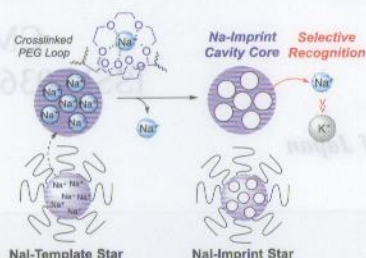


Heme is a typical and common prosthetic group for various kinds of proteins, which is utilized for active centers in many biologically important processes in vivo. However, heme has also been shown to function as a signaling molecule that regulates the functions of the proteins, suggesting that novel signaling cascades mediated by heme. We focused on the spectroscopic characterization of such “heme-regulated” proteins showing the unique heme environmental structures.

Chem. Lett. 2014, 43 1680–1689 doi:10.1246/cl.140787

Core-imprinted Star Polymers via Living Radical Polymerization: Precision Cavity Microgels for Selective Molecular Recognition

Takaya Terashima,* Hironori Kojima, and Mitsuo Sawamoto*

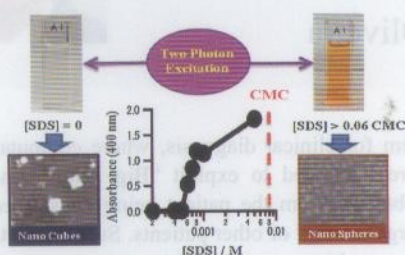


Na-imprinted PEG cavities were successfully created within microgel cores of star polymers for selective recognition of sodium cation over potassium cation. Such core-imprinted star polymers are efficiently synthesized by ruthenium-catalyzed linking reaction of PMMA arms with NaI template-bearing poly(ethylene glycol) (PEG) dimethacrylate, followed by the removal of the sodium template.

Chem. Lett. 2014, 43 1690–1692 doi:10.1246/cl.140605

Effect of Sodium Dodecyl Sulfate on the Formation of Silver Nanoparticles by Biphotonic Reduction of Silver Nitrate in Water

Umair Y. Qazi, Shinji Kajimoto, and Hiroshi Fukumura*

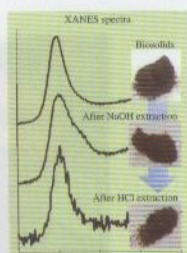


Nanoparticles were produced with nonfocused UV laser irradiation to an aqueous solution of silver-nitrate. Nanocubes were major products without SDS, whereas monodispersed nanospheres were formed when a SDS concentration was above a certain limit. This limit concentration was about ten times lower than CMC, suggesting that hemi-micellar adsorption of SDS on silver surfaces is a key to fabricate nanospheres.

Chem. Lett. 2014, 43 1693–1695 doi:10.1246/cl.140617

Assessment of Hedley's Sequential Extraction Method for Phosphorus Forms in Biosolids Using P K-edge X-ray Absorption Near-edge Structure Spectroscopy

Akira Takamoto and Yohey Hashimoto*

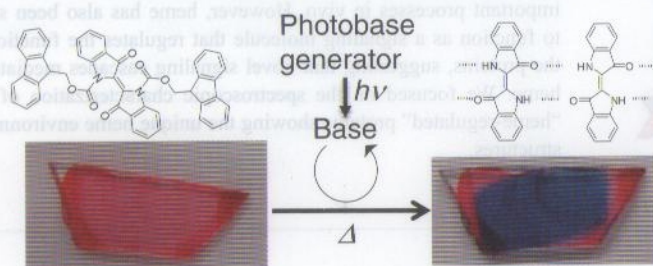


We determined phosphorus (P) species in biosolids and their residues after applying Hedley's sequential extractions using P K-edge XANES spectroscopy. The XANES technique was essential to identify secondary P phases in biosolids, which could not be detected by an XRD technique. Recalcitrant P associated with Fe minerals in biosolids could not completely be extracted by an NaOH fluid.

Chem. Lett. 2014, 43 1696–1697 doi:10.1246/cl.140526

Photoinduced Pigmentation Using Base-reactive Indigo Precursors in a Polymer Film

Koji Arimitsu,* Ryousuke Yamamoto, Midori Arai, and Masahiro Furutani

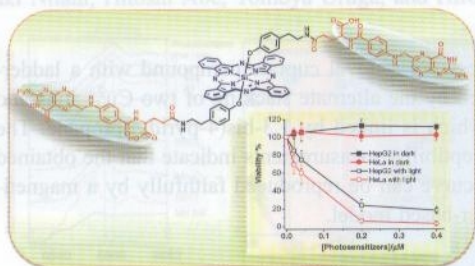


We have synthesized a soluble base-reactive indigo precursor as a latent pigment which regenerates an indigo molecule as a result of a base-catalyzed reaction. We also report here pigmentation of indigo molecules regenerated by the basic species from photobase generator in a polystyrene film.

Chem. Lett. 2014, 43 1698–1700 doi:10.1246/cl.140565

A Silicon(IV) Phthalocyanine–Folate Conjugate as an Efficient Photosensitizer

Yi-Wen Zheng, Shao-Fang Chen, Bi-Yuan Zheng, Mei-Rong Ke, and Jian-Dong Huang*

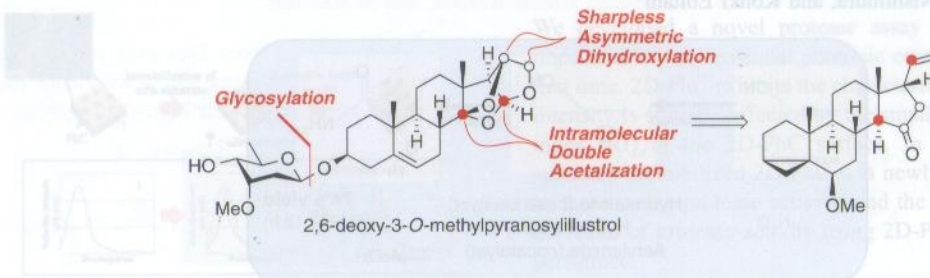


The novel silicon(IV) phthalocyanine axially conjugated with two molecules of folic acid has been prepared and characterized. This conjugate shows high photodynamic activities toward HeLa human cervical carcinoma cells ($IC_{50} = 0.071 \mu M$), which is slightly higher than that of HepG2 human hepatocellular carcinoma cells ($IC_{50} = 0.118 \mu M$).

Chem. Lett. 2014, 43 1701–1703 doi:10.1246/cl.140607

Total Synthesis of 2,6-Dideoxy-3-*O*-methylpyranosyllillustrol, a Seco-norpregnaneglycoside from *Mandevilla illustris*

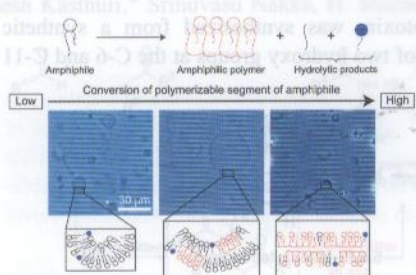
Minoru Tamiya,* Nobuhisa Isaka, Kazuya Ishizawa, Mayu Ikeda, and Masaji Ishiguro*



Chem. Lett. 2014, 43 1704–1706 doi:10.1246/cl.140632

Giant Vesicle Formation of Novel Polymerizable Amphiphile Associated with Its Polymerization and Hydrolysis in Water

Taisuke Banno, Yuki Kazayama, and Taro Toyota*

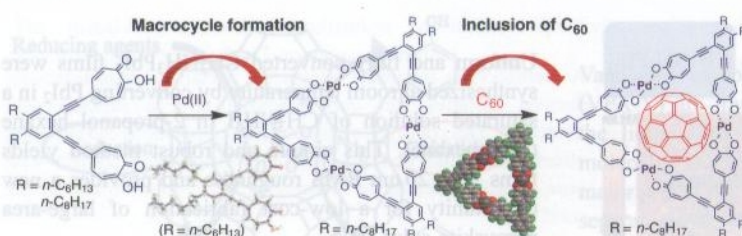


In an aqueous dispersion of a novel polymerizable amphiphile containing hydrolyzable linkages, spherical or tubular giant vesicles were formed after the polymerization reaction even though the hydrolysis of the amphiphile also occurred. This is probably due to the stabilization of the membrane structure composed of various amphiphiles, produced through the polymerization of the amphiphile.

Chem. Lett. 2014, 43 1707–1709 doi:10.1246/cl.140635

Synthesis of a Trinuclear Tropone–Palladium(II) Macrocycle and Its C_{60} Inclusion Properties

Hiroyuki Otani,* Chisaki Sumi, Hideyuki Shimizu, Masashi Hasegawa, and Masahiko Iyoda*

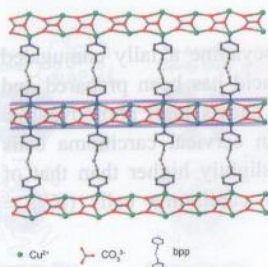


Trinuclear tropone–palladium(II) macrocycle having an inner cavity just large enough to include fullerene C_{60} was synthesized. Although the tropone–palladium(II) complex incompletely incorporated C_{60} in solution owing to weak interactions between the bis(tropone)–palladium(II) moieties and C_{60} , it formed an inclusion complex with C_{60} in the solid state.

Chem. Lett. 2014, 43 1710–1712 doi:10.1246/cl.140638

A Cuprate Spin Ladder Linked by a Pyridyl Ligand

Xiao Zhang, Sadafumi Nishihara,* Yuki Nakano, Kseniya Yu. Maryunina, and Katsuya Inoue*



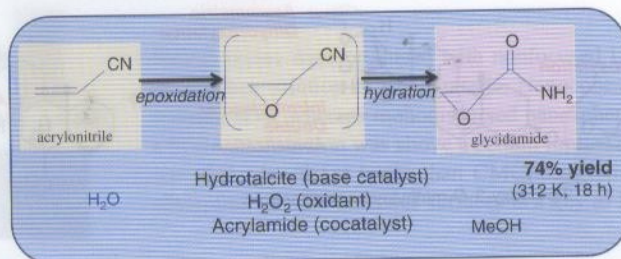
We succeeded in synthesizing a novel cuprate compound with a ladder-like configuration formed by the alternate stacking of two Cu²⁺ ions and a CO₃²⁻ ion, each of which is linked by 1,3-bis(4-pyridyl)propane. The results of magnetic susceptibility measurements indicate that the obtained magnetic susceptibility curve can be reproduced faithfully by a magnetically isolated spin ladder-based model.

Chem. Lett. 2014, 43 1713–1715 doi:10.1246/cl.140657

Editor's Choice

Synthesis of Glycidamide from Acrylonitrile Using Basic Hydrotalcite Catalyst in the Presence of Aqueous Hydrogen Peroxide and Unsaturated Amide

Shinpei Fujiwara, Shun Nishimura, and Kohki Ebitani*

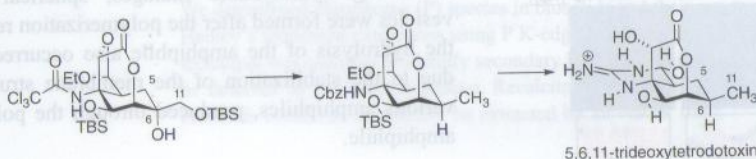


Chem. Lett. 2014, 43 1716–1718 doi:10.1246/cl.140658

Synthesis of 5,6,11-Trideoxytetradotoxin

Masaatsu Adachi, Ryo Sakakibara, Yoshiki Satake, Minoru Isobe, and Toshio Nishikawa*

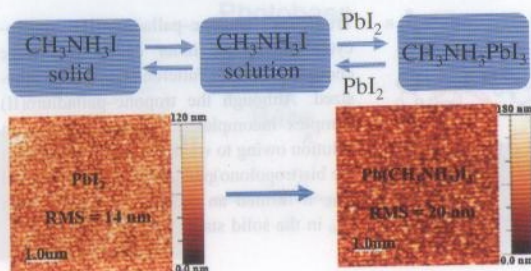
5,6,11-Trideoxytetradotoxin, a naturally occurring analogue of tetradotoxin, was synthesized from a synthetic intermediate of 5-deoxytetradotoxin by continuous radical deoxygenation of two hydroxy groups at the C-6 and C-11 positions.



Chem. Lett. 2014, 43 1719–1721 doi:10.1246/cl.140684

Fabrication of Lead Halide Perovskite Film by Controlling Reactivity at Room Temperature in Mixed Solvents

Yi Jin and George Chumanov*

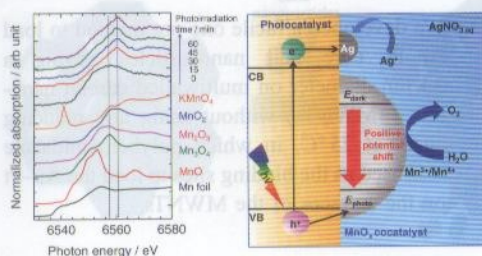


Uniform and fully converted CH₃NH₃PbI₃ films were synthesized at room temperature by converting PbI₂ in a saturated solution of CH₃NH₃I in 2-propanol-hexane (cyclohexane). This simple and robust method yields films with 20 nm RMS roughness and provides a new opportunity for a low-cost fabrication of large-area perovskite solar cells.

Chem. Lett. 2014, 43 1722–1724 doi:10.1246/cl.140644

In Situ XAFS Study of the Photoinduced Potential Shift of a MnO_x Cocatalyst on a SrTiO_3 Photocatalyst

Masaaki Yoshida,* Narihiro Gon, Saaya Maeda, Takehiro Mineo, Kiyofumi Nitta, Kazuo Kato, Hiroaki Nitani, Hitoshi Abe, Tomoya Uruga, and Hiroshi Kondoh

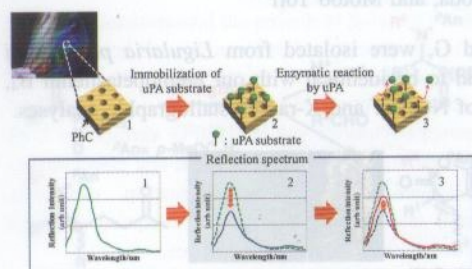


In situ XAFS spectra of a $\text{MnO}_x/\text{SrTiO}_3$ photocatalyst were acquired during an oxygen evolution reaction from an aqueous AgNO_3 solution. During this photocatalytic reaction, the absorption edge of the Mn K-edge XAFS spectrum shifted to higher energy values, suggesting that the electronic state of the MnO_x cocatalyst was changed by a positive potential shift via the migration of photoexcited holes.

Chem. Lett. 2014, 43 1725–1727 doi:10.1246/cl.140666

Development of Novel Protease Assay Device Using a Nanoimprinted Two-dimensional Photonic Crystal

Wakana Hashimoto, Tatsuro Endo,* Kenji Sueyoshi, and Hideaki Hisamoto

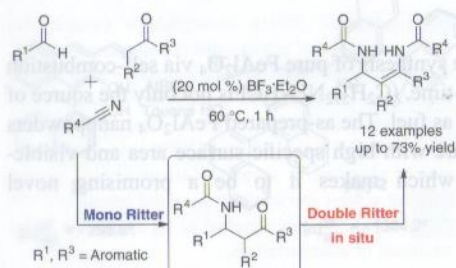


We developed a novel protease assay device using nanoimprinted two-dimensional photonic crystal (2D-PhC) for the first time. 2D-PhC exhibits the characteristic reflection, and its intensity is strongly affected by the small change in refractive index (RI) of the 2D-PhC surface. In this study, protease substrate-immobilized 2D-PhC was newly developed in order to measure the protease activity, and the simple and selective detection of protease activity using 2D-PhC was successfully performed.

Chem. Lett. 2014, 43 1728–1730 doi:10.1246/cl.140674

 $\text{BF}_3 \cdot \text{Et}_2\text{O}$ -catalyzed One-pot Synthesis of N,N' -(2-Alkyl-1,3-diarylprop-1-ene-1,3-diyl)diacetamides through a Tandem Aldol–Double Ritter-type Reaction

Mahesh Kasthuri,* Srinivasu Nakka, H. Sharath Babu, Ch. Sudhakar, M. Venkatanarayana, and P. V. Nagendra Kumar

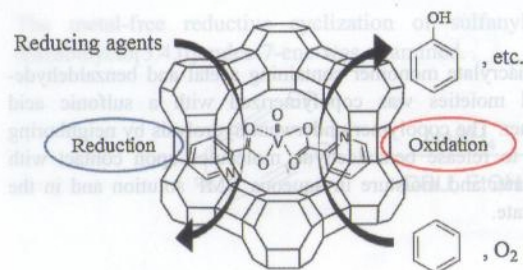


An atom and step economic synthesis of multifunctional N,N' -(2-alkyl-1,3-diarylprop-1-ene-1,3-diyl)diacetamides employing a multicomponent tandem aldol–double Ritter-type one-pot reaction between aromatic aldehydes and enolizable ketones and a nitrile source in the presence of 20 mol % of $\text{BF}_3 \cdot \text{Et}_2\text{O}$ is described. The reaction boosts operational simplicity, shorter reaction time, and simple work-up.

Chem. Lett. 2014, 43 1731–1733 doi:10.1246/cl.140634

Liquid-phase Oxidation of Benzene with Molecular Oxygen over Vanadium Complex Catalysts Encapsulated in Y-Zeolite

Atsushi Okemoto, Yoshiki Inoue, Koichi Ikeda, Chiaki Tanaka, Keita Taniya, Yuichi Ichihashi,* and Satoru Nishiyama

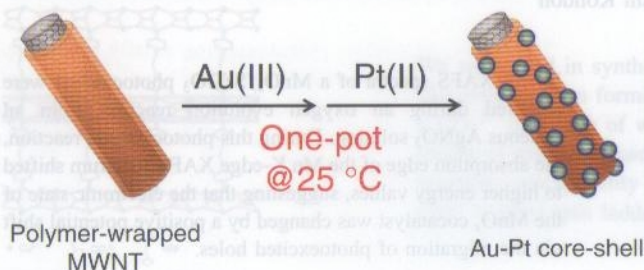


Vanadium complex catalysts encapsulated in Y-zeolite (VPA-Y) are investigated as heterogeneous catalysts for the liquid-phase oxidation of benzene to phenol with molecular oxygen and a reducing agent. Phenol is the major product of the process, and the catalyst can be easily separated from the product solution after the reaction.

Chem. Lett. 2014, 43 1734–1736 doi:10.1246/cl.140646

One-pot Synthesis of Gold–Platinum Core–Shell Nanoparticles on Polybenzimidazole-decorated Carbon Nanotubes

ChaeRin Kim, Tsuyohiko Fujigaya,* and Naotoshi Nakashima*



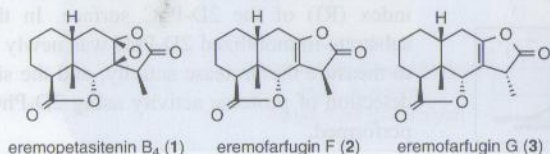
We developed a facile one-pot method to load Au–Pt core–shell nanoparticles having a 3.8 nm diameter on multiwalled carbon nanotubes (MWNTs) without using any reducing agent at 25 °C, in which polybenzimidazole was used as the binding sites to load the Au–Pt on the surfaces of the MWNTs.

Chem. Lett. 2014, 43 1737–1739 doi:10.1246/cl.140663

Isolation and Structure of Three Bislactones, Eremopetasitenin B₄ and Eremofarugins F and G, from *Ligularia przewalskii* and Revision of the Structure of an Epoxy-lactone Isolated from *Ligularia intermedia*

Yoshinori Saito, Aya Kamada, Yasuko Okamoto, Xun Gong, Chiaki Kuroda, and Motoo Tori*

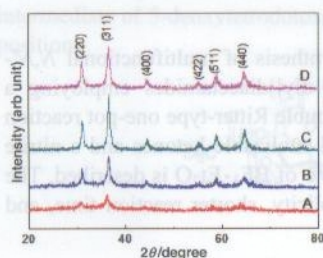
Three bislactones, eremopetasitenin B₄ and eremofarugins F and G, were isolated from *Ligularia przewalskii* collected in China, and the one already reported in 1997 was found to be identical with our eremopetasitenin B₄, which should be revised to have 11 α -H configuration on the basis of NOESY and X-ray crystallographic analyses.



Chem. Lett. 2014, 43 1740–1742 doi:10.1246/cl.140745

Facile Ionic Liquid Combustion Synthesis and Visible-light Photocatalytic Ability of Mesoporous FeAl₂O₄ with High Specific Surface Area

Mei-juan Chai, Xiang-min Chen, Ye Zhao, Rui-hong Liu, Jun Zhao, and Fa-tang Li*

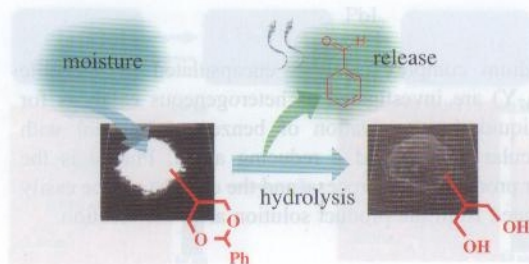


This research offers a facile synthesis of pure FeAl₂O₄ via self-combustion of ionic liquids for the first time. (C₂H₅)₂NH·HCl is not only the source of cation in IL but also serves as fuel. The as-prepared FeAl₂O₄ nanopowders exhibit mesoporous structure with high specific surface area and visible-light absorption ability, which makes it to be a promising novel photocatalyst.

Chem. Lett. 2014, 43 1743–1745 doi:10.1246/cl.140711

Water- and Moisture-sensitive Polymeric Releasing System by Hydrolysis of Acetal Moieties Coexisting with Acidic Units

Hiroshi Morikawa,* Dai Motegi, Kensuke Umemiya, Saki Watanabe, Hisatoyo Morinaga, and Suguru Motokucho

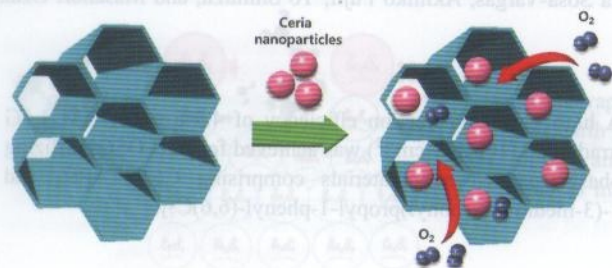


A methacrylate monomer containing acetal and benzaldehyde-derived moieties was copolymerized with a sulfonic acid monomer. The copolymer underwent hydrolysis by neighboring effects to release benzaldehyde molecules upon contact with pure water and moisture in aqueous DMF solution and in the solid state.

Chem. Lett. 2014, 43 1746–1748 doi:10.1246/cl.140717

Fabrication of Ceria Nanoparticles Incorporated in Porous Coordination Polymer

Cho Rong Kim, Takashi Uemura,* and Susumu Kitagawa*

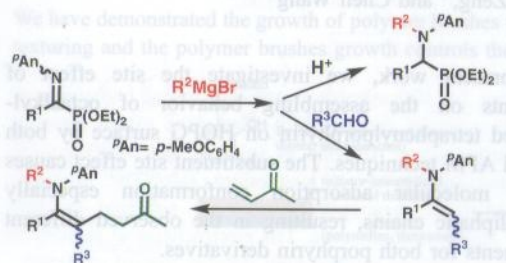


Nanosized ceria was fabricated in the channels of a porous coordination polymer (PCP) by the sol-gel polycondensation of cerium tetraisopropoxide. The resulting composite was characterized by IR, UV-vis, XRD, and XPS measurements, and the obtained ceria was found to be composed of a higher concentration of Ce^{3+} as compared to that of bulk synthesized ceria. Gas sorption of the composite showed the presence of ceria nanoparticles inside the channels of the PCP, which gave oxygen affinity for the PCP.

Chem. Lett. 2014, 43 1749–1751 doi:10.1246/cl.140719

N-Alkylation of α -Iminophosphonates and Application to Horner–Wadsworth–Emmons Reaction

Makoto Shimizu,* Masasato Tateishi, and Isao Mizota

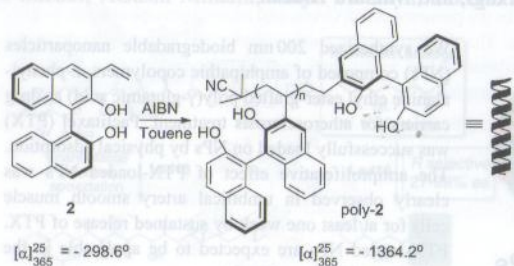


N-Alkylation of α -iminophosphonates with Grignard reagents gives α -N-alkylaminophosphonates. A subsequent Horner–Wadsworth–Emmons reaction of the intermediary α -metalated phosphonate takes place with aldehydes to give enamines. The enamine thus prepared reacts with MVK to give a four-component coupling product.

Chem. Lett. 2014, 43 1752–1754 doi:10.1246/cl.140763

Optically Active Helical Polymer from Radical Polymerization of (S)-3-Vinyl-2,2'-dihydroxy-1,1'-binaphthyl

Yehui Chen, Liwen Yang, Nianfa Yang,* and Zhusheng Yang



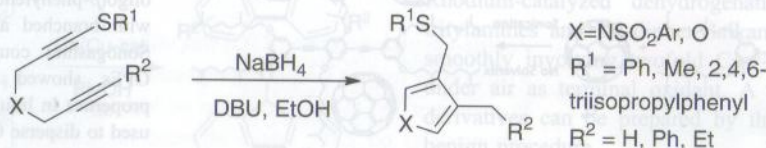
(S)-3-Vinyl-2,2'-dihydroxy-1,1'-binaphthyl (2) ($[\alpha]_{365}^{25} = -298.6^\circ$) was synthesized and radically polymerized using AIBN as an initiator to obtain poly-2 ($[\alpha]_{365}^{25} = -1364.2^\circ$) which has been proved to take one-handed helical backbone in solution.

Chem. Lett. 2014, 43 1755–1757 doi:10.1246/cl.140755

Metal-free Reductive Cyclization and Isomerization of Sulfanyl-1,6-diynes Using Sodium Borohydride

Yukiteru Ito and Mitsuhiro Yoshimatsu*

The metal-free reductive cyclization of sulfanyl-1,6-diynes with sodium borohydride in the presence of diazabicyclo[5.4.0]undec-7-ene was examined.

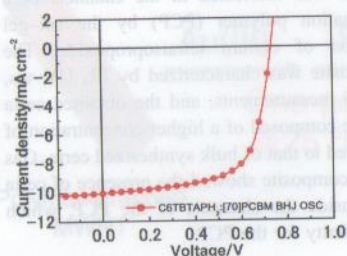


X = NSO_2Ar , O
 R^1 = Ph, Me, 2,4,6-triisopropylphenyl
 R^2 = H, Ph, Et

Chem. Lett. 2014, 43 1758–1760 doi:10.1246/cl.140688

Octahexyltetraabenzotriazaporphyrin: A Discotic Liquid Crystalline Donor for High-performance Small-molecule Solar Cells

Quang-Duy Dao,* Koichi Watanabe, Hiromichi Itani, Lydia Sosa-Vargas, Akihiko Fujii, Yo Shimizu, and Masanori Ozaki*

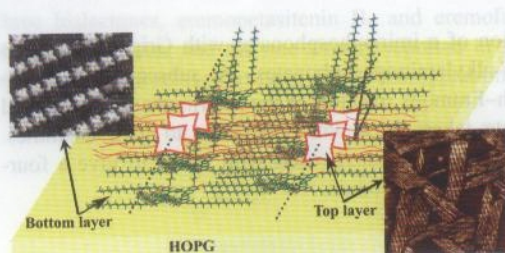


A high power conversion efficiency of 4.9% under AM 1.5G irradiation (100 mW cm^{-2}) was achieved for BHJ OSCs utilizing phase-separated nanomaterials comprising C6BTAPH₂ and 1-(3-methoxycarbonyl)propyl-1-phenyl-(6,6)C₇₁.

Chem. Lett. 2014, 43 1761–1763 doi:10.1246/cl.140685

Substituent Site Effect Induced Assemblies of Porphyrin Derivatives on Graphite Surface Characterized Using a Scanning Probe Microscope

Min Li, Haijun Xu, Yanlian Yang, Lina Zhao, Zhen Shen,* Qingdao Zeng,* and Chen Wang*

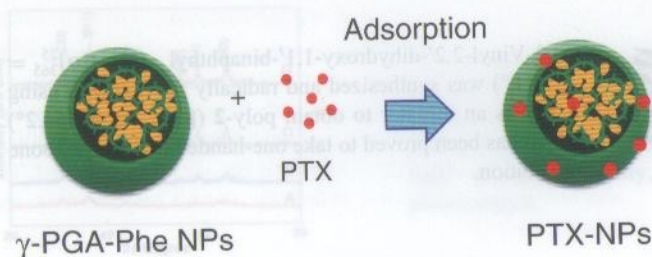


In the present work, we investigate the site effect of substituents on the assembling behavior of octaalkyl-substituted tetraphenylporphyrin on HOPG surface by both STM and AFM techniques. The substituent site effect causes different molecular adsorption conformation especially among aliphatic chains, resulting in the observed different arrangements for both porphyrin derivatives.

Chem. Lett. 2014, 43 1764–1766 doi:10.1246/cl.140687

Sustainable Release of Paclitaxel from Biodegradable Poly(γ -glutamic acid) Nanoparticles for Treatment of Atherosclerosis

Paninee Chetprayoon, Fumiaki Shima, Michiya Matsusaki, Takami Akagi, and Mitsuru Akashi*

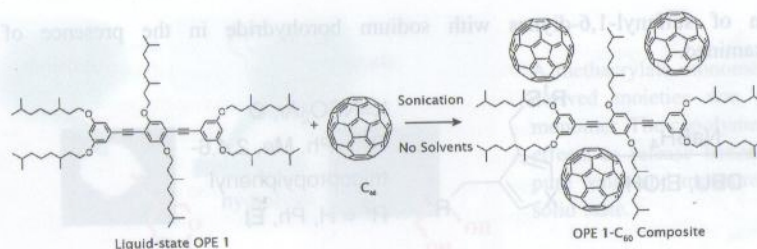


We synthesized 200 nm biodegradable nanoparticles (NPs) composed of amphipathic copolymers, L-phenyl-alanine ethyl ester-grafted poly(γ -glutamic acid) as drug carriers for atherosclerosis treatment. Paclitaxel (PTX) was successfully loaded on NPs by physical adsorption. The antiproliferative effect of PTX-loaded NPs was clearly observed in umbilical artery smooth muscle cells for at least one week by sustained release of PTX. PTX-loaded NPs are expected to be applicable in the treatment of atherosclerosis.

Chem. Lett. 2014, 43 1767–1769 doi:10.1246/cl.140736

Dispersion of Fullerene in Neat Synthesized Liquid-state Oligo(*p*-phenyleneethynylene)s

Naoya Adachi,* Ryo Itagaki, Masafumi Sugeno, and Takayuki Norioka

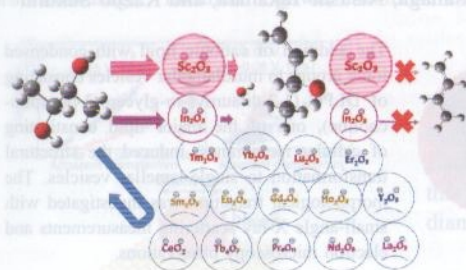


We have synthesized liquid-state oligo(*p*-phenyleneethynylene)s (OPEs) with branched alkyl side chains by Sonogashira coupling reaction. The OPEs showed strong fluorescence properties in liquid state and could be used to disperse C₆₀.

Chem. Lett. 2014, 43 1770–1772 doi:10.1246/cl.140587

Vapor-phase Catalytic Dehydration of 2,3-Butanediol into 3-Buten-2-ol over Sc_2O_3

Hailing Duan, Yasuhiro Yamada, and Satoshi Sato*



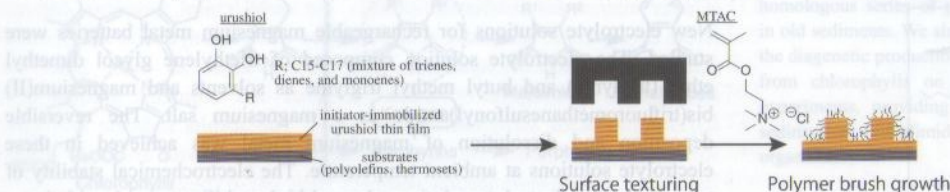
In the vapor-phase catalytic dehydration of 2,3-butanediol over rare earth oxides, Sc_2O_3 converted 2,3-butanediol into 3-buten-2-ol with an excellent selectivity of 85.0% at 99.9% conversion as well as In_2O_3 .

Chem. Lett. 2014, 43 1773–1775 doi:10.1246/cl.140662

Polymer Brush Growth from Surface-textured Thin Urushiol Films

Hirohmi Watanabe,* Aya Fujimoto, Rika Yamamoto, Jin Nishida, Yuji Higaki, and Atsushi Takahara*

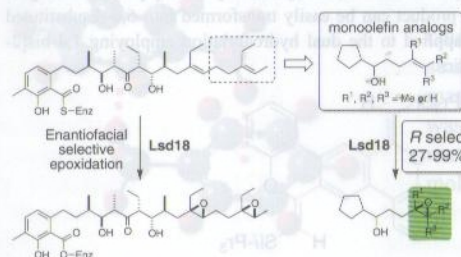
We have demonstrated the growth of polymer brushes from a surface-textured thin urushiol film. The combination of surface texturing and the polymer brushes growth controls the surface topography as well as surface physicochemical properties.



Chem. Lett. 2014, 43 1776–1778 doi:10.1246/cl.140670

Analysis of Enantiofacial Selective Epoxidation Catalyzed by Flavin-containing Monooxygenase Lsd18 Involved in Ionophore Polyether Lasalocid Biosynthesis

Gaku Suzuki, Atsushi Minami, Mayu Shimaya, Takeshi Kodama, Yoshiki Morimoto, Hiroki Oguri, and Hideaki Oikawa*

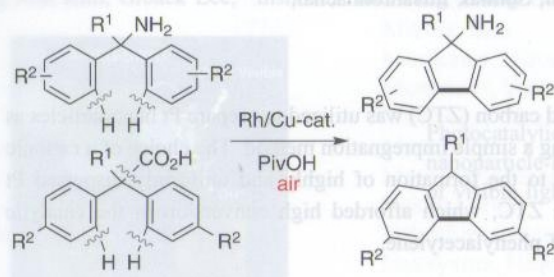


Biotransformation study utilizing structurally simplified monoolefin analogs with different substitution patterns on the olefin moiety revealed important structural requirements for enantiofacial selectivity of Lsd18-catalyzed epoxidation involved in ionophore polyether lasalocid biosynthesis.

Chem. Lett. 2014, 43 1779–1781 doi:10.1246/cl.140721

Rhodium-catalyzed Intramolecular Dehydrogenative Aryl–Aryl Coupling Using Air as Terminal Oxidant

Hannah Baars, Yuto Unoh, Takeshi Okada, Koji Hirano, Tetsuya Satoh,* Ken Tanaka, Carsten Bolm, and Masahiro Miura*

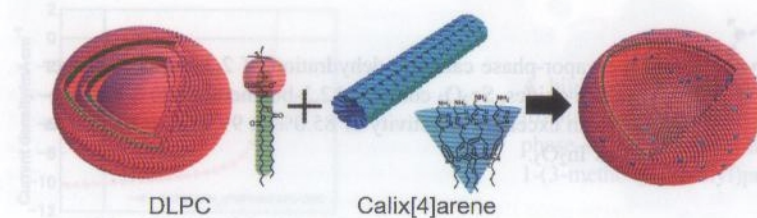


Rhodium-catalyzed dehydrogenative cyclization of tritylamines and 2,2-diphenylalkanoic acids proceeds smoothly involving twofold $\text{Csp}^2\text{–H}$ bond cleavages under air as terminal oxidant. A variety of fluorene derivatives can be prepared by the environmentally-benign procedure.

Chem. Lett. 2014, 43 1782–1784 doi:10.1246/cl.140690

Transformation from Multi- to Single-lamellar Vesicle by Addition of a Cationic Lipid to 1,2-Dilauroyl-*sn*-glycero-3-phosphocholine Explored with SAXS and TEM

Genki Kubo, Shunsuke Sakamoto, Shota Fujii, Yusuke Sanada, Takuo Yasunaga, Atsushi Takahara, and Kazuo Sakurai*

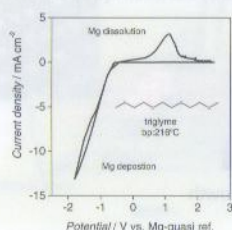


The addition of cationic lipid with condensed ionic groups to multilamellar vesicles consisting of DLPC (1,2-dilauroyl-*sn*-glycero-3-phosphocholine), one of the major lipid constituting of cellular membranes, induced the structural transformation to single-lamellar vesicles. The morphological transition was investigated with small-angle X-ray scattering measurements and electron microscopy observations.

Chem. Lett. 2014, 43 1785–1787 doi:10.1246/cl.140668

New Magnesium-ion Conductive Electrolyte Solution Based on Triglyme for Reversible Magnesium Metal Deposition and Dissolution at Ambient Temperature

Tomokazu Fukutsuka, Keisuke Asaka, Akane Inoo, Ryohei Yasui, Kohei Miyazaki, Takeshi Abe,* Koji Nishio, and Yoshiharu Uchimoto



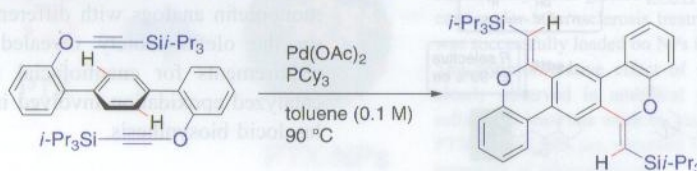
New electrolyte solutions for rechargeable magnesium metal batteries were studied. The electrolyte solution composed of triethylene glycol dimethyl ether (triglyme) and butyl methyl triglyme as solvents and magnesium(II) bis(trifluoromethanesulfonyl)amide as a magnesium salt. The reversible deposition and dissolution of magnesium metal was achieved in these electrolyte solutions at ambient temperature. The electrochemical stability of triglyme-based electrolyte solutions showed high stability toward oxidation.

Chem. Lett. 2014, 43 1788–1790 doi:10.1246/cl.140704

Palladium-catalyzed Annulation of 2-Substituted Silylethynoxybiaryls through δ -C–H Activation

Yasunori Minami,* Tomohiro Anami, and Tamejiro Hiyama*

The intramolecular hydroarylation of 2-(silylethynoxy)biphenyls proceeded in the presence of $\text{Pd}(\text{OAc})_2$ and tricyclohexylphosphine to give 6-methylene-6*H*-dibenzo[*b,d*]pyrans in high yields via σ -C–H bond cleavage. The product can be easily transformed into 6,6-disubstituted dibenzopyrans via protodesilylation, followed by 1,2-addition. The reaction was applied to the dual hydroarylation employing 1,4-bis[2-(triisopropylsilylethynoxy)phenyl]benzene to form pentacyclic condensed aromatics.

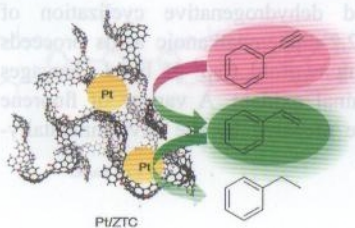


Chem. Lett. 2014, 43 1791–1793 doi:10.1246/cl.140725

Editor's Choice

Preparation of Highly Dispersed Pt Nanoparticles Supported on Zeolite-templated Carbon and Catalytic Application in Hydrogenation Reaction

Chuanxia Jiang, Kenji Hara, Kotaro Namba, Hirokazu Kobayashi, Somlak Ittisanronnachai, Hiroto Nishihara, Takashi Kyotani, and Atsushi Fukuoka*



Zeolite-templated carbon (ZTC) was utilized to prepare Pt nanoparticles as a support by using a simple impregnation method. The choice of a cationic Pt precursor led to the formation of highly and uniformly dispersed Pt nanoparticles on ZTC, which afforded high conversion in the catalytic hydrogenation of phenylacetylene.

Chem. Lett. 2014, 43 1794–1796 doi:10.1246/cl.140699